Chiral Bands, Dynamical Spontaneous Symmetry Breaking, and the Selection Rule for Electromagnetic Transitions in the Chiral Geometry

Chiral Bands, Dynamical Spontaneous Symmetry Breaking, and the Selection Rule for Electromagnetic Transitions in the Chiral Geometry

T. Koike,[1] K. Starosta,[1,2] and I. Hamamoto[3,4]

[1]*Department of Physics and Astronomy, SUNY at Stony Brook, New York 11794, USA*
[2]*Department of Physics and Astronomy and National Superconducting Cyclotron Laboratory, MSU, East Lansing, Michigan 48824, USA*
[3]*Division of Mathematical Physics, LTH, University of Lund, Sweden*
[4]*The Niels Bohr Institute, Blegdamsvej 17, Copenhagen Ø, DK 2100, Denmark*

(Received 16 March 2004; revised manuscript received 29 July 2004; published 22 October 2004)

A model for a special configuration in triaxial odd-odd nuclei is constructed which exhibits degenerate chiral bands with a sizable rotation, a manifestation of dynamical spontaneous symmetry breaking. A quantum number obtained from the invariance of the model Hamiltonian, which characterizes observable states, is given and selection rules for electromagnetic transition probabilities in chiral bands is derived in terms of this quantum number. The degeneracy of the lowest two bands is indeed obtained in the numerical diagonalization of the Hamiltonian at an intermediate spin range, over which electromagnetic transitions follow exactly the selection rule expected for the chiral geometry.

DOI: 10.1103/PhysRevLett.93.172502 PACS numbers: 23.20.Lv, 21.10.Re, 21.60.Ev

Spontaneous symmetry breaking is an important phenomenon in a physical system, various forms of which have been observed in nature. In particular, spontaneous formation of handedness or chirality is a subject of general interest in molecular physics, the characterization of elementary particles, and in optical physics. The occurrence of chirality in a nuclear structure has recently been considered theoretically [1,2] and experimental spectra exhibiting the predicted patterns have been reported [3,4]. The present work is an attempt to further develop the theory of nuclear chirality through the identification of selection rules that can occur in the electromagnetic transitions in chiral rotational bands.

As in many other systems existing in nature, the total Hamiltonian for the nuclear system is taken to be invariant under the exchange of the right- and left-handed geometry. Chirality in triaxial nuclei is characterized by the presence of three angular-momentum vectors, which are generally noncoplanar and thereby make it possible to define chirality. An example is shown in Fig. 1. The hallmark of nuclear chirality is the observation of two almost degenerate $\Delta I = 1$ rotational bands [3,4], chiral bands, having the same parity. Those almost degenerate states do not appear around the ground state or the rotational bandhead, but they are observed only after a sufficient amount of collective rotation develops. The exact degeneracy translates to vanishing matrix elements which connect the right- and left-handed systems. Though the observed near degeneracy of the two bands is a primary indication of chiral geometry, this geometry can be pinned down in a more definitive way if electromagnetic transition probabilities expected for the chiral bands are experimentally confirmed. Because of the complexity and generality of nuclear chirality, the behavior of electromagnetic transition probabilities or the selection rules are not yet understood. To address this issue, a limiting case of the particle-rotor model has been sought in the present study. In our opinion an application of this special theoretical limit outweighs a loss of generality.

This Letter reports a study of a simple model for a special configuration in triaxial odd-odd nuclei, which simulates the configuration of nearly degenerate bands observed in several nuclei with $N \approx 75$ [3]. In this special case, an additional symmetry exists and thus a quantum number in the model Hamiltonian can be obtained. Utilizing this quantum number allows for derivation of the selection rule for electromagnetic transitions in an unambiguous manner. Subsequently the formation of chiral geometry with the selection rule is numerically confirmed.

First we write down the Hamiltonian of the particle-rotor model [5] appropriate for triaxial odd-odd nuclei and the symmetry (or a quantum number) of the

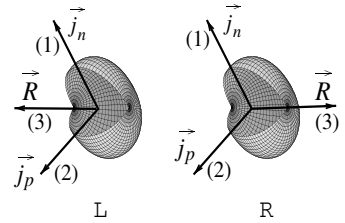

FIG. 1. Sketch of the idealized chiral geometry. The core, proton, and neutron angular momenta denoted by $\vec{R}$, $\vec{j}_p$, and $\vec{j}_n$, respectively, are almost parallel to the principal axes of the triaxial body, which are labeled by the numbers inside parentheses. The right-handed system is denoted by R, while the left-handed one by L.

Hamiltonian is examined. The current model consists of a triaxially deformed core with $\gamma = 90°$ coupled to one proton particle and one neutron hole in the same single-j shell. The statement "rotation with $\gamma = 90°$" is equivalent to "the $\gamma = -30°$ rotation" in the Lund convention [6] except that the intermediate axis is the quantization axis (3-axis). Denoting the components of the core angular momentum $\vec{R}$ along the long, short, and intermediate axes of the triaxial body as R_1, R_2, and R_3, respectively, the rotational Hamiltonian of the core is

$$H_{\rm rot} = \frac{\hbar^2}{8J_0}[R_3^2 + 4(R_1^2 + R_2^2)], \tag{1}$$

where the hydrodynamical moments of inertia are assumed. Since the kinetic energy operator of particles is isotropic, we need not discuss it here in relation to the symmetry. In the case of a single-j-shell configuration the well-known triaxially deformed quadrupole potential

$$V(r, \theta, \phi) \propto \beta k(r)\Big[Y_{20}(\theta, \phi)\cos(\gamma) + \frac{1}{\sqrt{2}}[Y_{22}(\theta, \phi) + Y_{2-2}(\theta, \phi)]\sin(\gamma)\Big] \tag{2}$$

can be written for $\gamma = 90°$ as

$$V_{sp}^{\pi} \propto (j_{p1}^2 - j_{p2}^2) \tag{3}$$

for the proton particle and as

$$V_{sp}^{\nu} \propto (j_{n2}^2 - j_{n1}^2) \tag{4}$$

for the neutron hole (see Ref. [7]), using the fact that the one-particle matrix elements of $(Y_{22} + Y_{2-2})$ are proportional to those of $(j_1^2 - j_2^2)$. In Eqs. (3) and (4) j_{p1} and j_{p2} (j_{n1} and j_{n2}) express the components of the proton (neutron) angular-momentum operator $\vec{j}_p$ ($\vec{j}_n$) along the long (1-) and short (2-) axes, respectively. We note that the potential for a hole is obtained by changing the sign of that for a particle. The proportionality constants in (3) and (4), which are positive and linearly dependent on deformation parameter β, are exactly the same, if protons and neutrons are in the same single-j shell.

The total Hamiltonian constructed from (1), (3), and (4) has D_2 symmetry so that the projection of the core rotation on the quantization axis characterized by quantum number R_3 takes only even integer values [5]. Moreover, the total Hamiltonian is invariant under the rotation by 90° or 270° about the 3-axis combined with an exchange of the valence proton and neutron. We denote this combined transformation by A, and the operator exchanging valence proton and neutron by C, while the rotations of interest are given by the operators

$$\exp\Big(i\frac{\pi}{2}R_3\Big) \quad \text{or} \quad \exp\Big(i\frac{3\pi}{2}R_3\Big). \tag{5}$$

The invariance of the total Hamiltonian under the A operator is a consequence of corresponding invariances of the rotor Hamiltonian given by Eq. (1) and single-particle potentials given by Eqs. (3) and (4). Indeed, for the rotor, the expression (1) is invariant under the exchange of R_1^2 with R_2^2 resulting from the rotation given by (5) and is unaffected by the C operation. For the single-particle potentials, the operator C exchanges the proton-particle potential with the neutron-particle potential, while the rotations given by (5) exchange j_{p1}^2 with j_{p2}^2 and j_{n1}^2 with j_{n2}^2. Then, the sum $V_{sp}^{\pi} + V_{sp}^{\nu}$ is invariant under the A operation.

Let us assign $C = +1$ and -1 to the components of the intrinsic neutron-proton wave functions which are symmetric and antisymmetric under the exchange of valence proton and valence neutron, respectively. The energy eigenstates are simultaneous eigenstates of the A operator having eigenvalues of $A = +1$ or -1; therefore, for the eigenstates with $A = +1$ the components with $R_3 = 0, \pm 4, \pm 8, \cdots$ which get $+1$ in the rotation of Eq. (5) must have $C = +1$, while those with $R_3 = \pm 2, \pm 6, \cdots$ which get -1 in the rotation of Eq. (5) have $C = -1$. On the other hand, for the eigenstates with $A = -1$ the components with $R_3 = 0, \pm 4, \pm 8, \cdots$ must have $C = -1$, while those with $R_3 = \pm 2, \pm 6, \cdots$ have $C = +1$.

If only the core contributions are taken into account for $E2$ transitions, we must have $\Delta C = 0$, in order to obtain nonvanishing transition probabilities, since the neutron and proton are spectators. Furthermore, $\gamma = 90°$ means that the $E2$ matrix elements with $\Delta R_3 = 0$ vanish (see Chap. 6B of Ref. [5]); therefore we must have $\Delta R_3 = \pm 2$. Then, $E2$ matrix elements vanish between the states with the same A values. This selection rule entails that static quadrupole moments always vanish in the present model.

For $M1$ transitions, the operator

$$(M1)_\mu = \sqrt{\frac{3}{4\pi}}\frac{e\hbar}{2mc}[(g_\ell - g_R)\ell_\mu + (g_s^{\rm eff} - g_R)s_\mu] \tag{6}$$

is nearly isovector if realistic parameters $(g_\ell - g_R) = 0.5$ (-0.5) and $(g_s^{\rm eff} - g_R) = 2.848$ (-2.792) for protons (neutrons) with $g_R = 0.5$ and $g_s^{\rm eff} = 0.6 g_s^{\rm free}$ are used. Therefore, $M1$ matrix elements between the components with the same C values are in general an order of magnitude smaller than those with the opposite sign of C. Considering that the $M1$ operator cannot connect the components with $\Delta R_3 \geq 2$, $M1$ transition matrix elements between the states with the same A values are an order of magnitude smaller than those with opposite A.

Summarizing the above results, the selection rule obtained in the present model is that $E2$ transitions between the states of the same A are forbidden, while $M1$ transitions between the same A are much weaker than those between the states of opposite A. This selection rule must work for any eigenstates of the present Hamiltonian, irrespective of whether the chiral geometry is achieved.

We note that the invariance of the total Hamiltonian and the selection rule for electromagnetic transitions described above also apply in the presence of pair correlation with a reasonable approximation, though we do not here go into detail.

The total angular momentum $\vec{I}$ is a sum of three vectors $\vec{I} = \vec{R} + \vec{j}_p + \vec{j}_n$. Examining the single-particle potentials (3) and (4), it is energetically favored if $\vec{j}_p$ points to the 2-axis while $\vec{j}_n$ points to the 1-axis. Since the energy of the core (1) is minimized for the rotation about the 3-axis, the angular momentum $\vec{R}$ of the core in the lowest-energy state starts to align with the 3-axis, as collective rotation increases. For sufficiently fast rotation, at which Coriolis force becomes dominant, both $\vec{j}_p$ and $\vec{j}_n$ also align with the 3-axis. Thus, for intermediate values of I, the three vectors $\vec{j}_n$, $\vec{j}_p$, and $\vec{R}$ will exhibit the right-handed geometry if the three vectors point to the positive direction of the 1-, 2-, and 3-axes, respectively. Conversely, when one or all of the three vectors point to the negative direction, they construct the left-handed geometry. The idealized chiral geometry is sketched in Fig. 1. The energies of the states associated with opposite handedness would be degenerate if there were no tunneling between the two; this is a spontaneous formation of chirality.

When chiral geometry is realized, observed two chiral-degenerate states may be written as [8]

$$|I+\rangle = \frac{1}{\sqrt{2}}(|IL\rangle + |IR\rangle), \tag{7}$$

$$|I-\rangle = \frac{i}{\sqrt{2}}(|IL\rangle - |IR\rangle), \tag{8}$$

where left- and right-handed geometry states are written as $|IL\rangle$ and $|IR\rangle$, respectively. For states with $I \gg 1$ it is expected that

$$\langle IL|E2|IR\rangle \approx 0 \quad \text{and} \quad \langle IL|M1|IR\rangle \approx 0, \tag{9}$$

where the electric-quadrupole and magnetic-dipole operators are denoted by $E2$ and $M1$, respectively. If $\approx$ in (9) is replaced by $=$, then within the pair of chiral bands

$$\begin{aligned} B(EM; I'+ \rightarrow I+) &= B(EM; I'- \rightarrow I-), \\ B(EM; I'+ \rightarrow I-) &= B(EM; I'- \rightarrow I+), \end{aligned} \tag{10}$$

where EM expresses either $E2$ or $M1$.

In the present model together with the chiral geometry described above, the exchange of the right-handed with left-handed systems can be equally obtained by the exchange of the valence neutron and proton while keeping the direction of $\vec{R}$ unchanged; see Fig. 1. Since the rotations (5) about the 3-axis do not affect chirality, the operation A exchanges $|IR\rangle$ with $|IL\rangle$. The formation of chirality means that the two nearly degenerate states $|I+\rangle$ and $|I-\rangle$ have different eigenvalues of A. We arrange the chiral bands so that the $\Delta I = 2$ $E2$ transitions are always allowed within the respective bands. Then, the sign of A in a given band must change at every increase of I by 2; see Fig. 2. A similar sequence of the quantum number in the yrast state was considered in the model described in Ref. [9], in which an odd high-j particle coupled to a $\gamma = -30°$ triaxial core.

In Fig. 2 the consequence of the present selection rules is illustrated for both interbands and intrabands $E2$ and $M1$ transitions with chiral geometry. The thick arrows indicate allowed $E2$ transitions and stronger $M1$ transitions. The thinner arrows are for the weaker $M1$ transitions. For $\Delta I = 1$ transitions the allowed $E2$ transitions occur together with stronger $M1$ transitions, since both types of transition need a change of A.

Now, our particle-rotor Hamiltonian is numerically diagonalized taking $j = h_{11/2}$ for both odd particles [10]. In order to simulate a chiral nucleus in the mass $A \sim 130$ region, the parameters $A = 130$, $Z = 55$, $\beta = 0.3$, and $J_0 = 8.55\ \hbar^2/\mathrm{MeV}$ are used. Experimental information on chiral bands in this mass region is indicated by observed energies (see, for instance, Refs. [3,11], and references therein). The results of calculations are shown in Fig. 3. At the lower spin region ($8 \leq I \leq 13$), the two bands are displaced in energy due to less defined chiral geometry with insufficient collective rotation. For $13 < I < 25$, the approximate degeneracy obtained for these bands is already a good sign of the realization of chiral geometry. In its ideal case, a sequence of perfectly degenerate states makes it impossible to identify two separated rotational bands based on the excitation energy only. However, the properties of electromagnetic transitions allow for a definitive distinction between the chiral partner bands. Therefore, in Fig. 3, the bands are organized based on energy at low spin and on $B(E2; I \rightarrow I-2)$ values over the degenerate spin range. The label of the

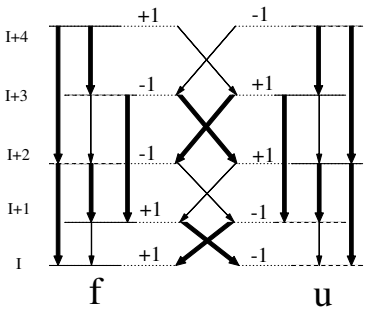

FIG. 2. Selection rule expected for both interbands and intrabands $E2$ and $M1$ transitions, when chiral geometry is realized in the present model. Allowed $E2$ transitions (with $\Delta I = 1$ and 2) and stronger $M1$ transitions (with $\Delta I = 1$) are indicated by thick arrows. Allowed but weaker $\Delta I = 1$ $M1$ transitions are indicated by thinner arrows. Solid lines represent states of $A = +1$, while the dashed lines those of $A = -1$. Two chiral pair bands are denoted by f and u.

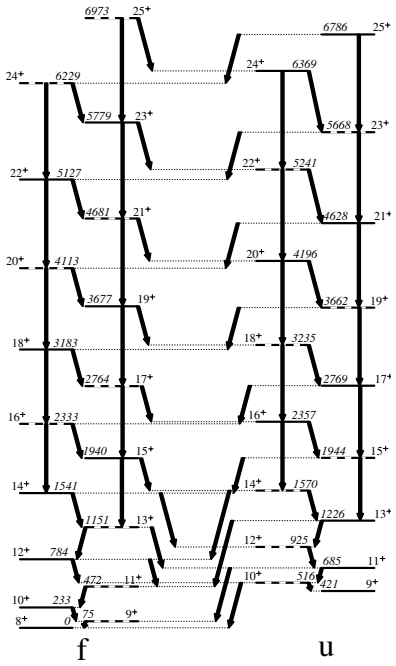

FIG. 3. Calculated level scheme for a pair of $\Delta I = 1$ bands. Arrows represent transitions of strong $B(E2)$ or $B(M1)$. The calculated $E2$ ($M1$) transitions, which are not shown in the figure, are totally forbidden (negligibly weak). Solid and dashed lines represent levels with $A = +1$ and -1, respectively, or vice versa. See text for detail.

bands f and u in Fig. 3 is hence given from the low spin behavior. Interpretations for the low spin region will be discussed in Ref. [10].

In the applied model, the total number of basis states for spin I is given by $(1/2)(I + 1/2)(2j_p + 1)(2j_n + 1)$, which is equal to 1116 for $I = 15$ for the $j_p \otimes j_n^{-1}$ configuration with $j_p = j_n = h_{11/2}$. Using the bases quantized along the intermediate axis of the triaxial shape (the 3-axis), only about ten states cover nearly 70% probabilities. Among those wave functions, it is found that the single-particle basis states are effectively all of those basis states, in which one proton particle and one neutron hole occupy the lowest and highest doubly degenerate single-particle levels, respectively, for $\gamma = 90°$. For the lowest pair bands the particle/hole states contribute about 98% to the total probability distribution near the bandhead, and this number reduces, with increasing spin, to $\sim$70% at $I = 15$. For this reason in the following calculation of electromagnetic transition probabilities a simplified model is used, in which one proton particle and one neutron hole are restricted to those lowest and highest levels in the $h_{11/2}$ shell, respectively.

The $B(E2; I \rightarrow I-2)$, $B(M1; I \rightarrow I-1)$, and $B(E2; I \rightarrow I-1)$ values of both interband and intraband transitions which are calculated using the simplified model are represented by thick arrows in Fig. 3. For $E2$ transitions, only the core contribution, which dominates over those from the valence proton and neutron, is taken into account, while for $M1$ transitions $g_R = 55/130 = 0.423$ and $g_s^{\rm eff} = 0.6 g_s^{\rm free}$ are used. The characteristic features, which are expected for the chiral bands as illustrated in Fig. 2, are reproduced exactly in Fig. 3. Namely, $A = +1, +1, -1, -1, +1, +1, -1, -1, \cdots$ in the $I = 14, 15, 16, 17, 18, 19, 20, 21, \cdots$ states of the f (or u) band, while the states of the u (or f) band have opposite sign of A. Weaker $M1$ transitions in this numerical example are practically forbidden transitions, and thus are not indicated in the figure.

Deviations of the actual situation in nuclei from the simple assumption made in the present model may modify the selection rule described above. Nevertheless, the interpretation presented in this Letter should serve as a starting point for the study of more complicated nuclear systems.

In conclusion, using a simple model which simulates two nearly degenerate bands observed in several odd-odd nuclei, a quantum number derived from the model Hamiltonian is used to obtain selection rules for electromagnetic transitions. The selection rule applied to the case of chiral geometry is reproduced by the numerical diagonalization of the Hamiltonian when the calculated two lowest $\Delta I = 1$ bands are almost degenerate.

One of the authors (I. H.) thanks I. Ragnarsson for the use of his computer program to check part of the present results. The authors express their sincere thanks to B. Mottelson for generous comments and a careful reading of the present manuscript.

[1] S. Frauendorf and J. Meng, Nucl. Phys. **A617**, 131 (1997).
[2] V. I. Dimitrov, S. Frauendorf, and F. Dönau, Phys. Rev. Lett. **84**, 5732 (2000).
[3] K. Starosta *et al.*, Phys. Rev. Lett. **86**, 971 (2001).
[4] C. Vaman *et al.*, Phys. Rev. Lett. **92**, 032501 (2004).
[5] A. Bohr and B. R. Mottelson, *Nuclear Structure* (Benjamin, Reading, MA, 1975), Vol. II.
[6] G. Andersson *et al.*, Nucl. Phys. **A268**, 205 (1976).
[7] I. Hamamoto and B. Mottelson, Phys. Lett. B **127**, 281 (1983); **132**, 7 (1983).
[8] K. Starosta, T. Koike, C. J. Chiara, D. B. Fossan, and D. R. LaFosse, Nucl. Phys. **A682**, 375c (2001).
[9] I. Hamamoto, Phys. Lett. B **193**, 399 (1987).
[10] T. Koike, K. Starosta, D. B. Fossan, C. Vaman, and I. Hamamoto (to be published).
[11] T. Koike, K. Starosta, C. J. Chiara, D. B. Fossan, and D. R. LaFossse, Phys. Rev. C **67**, 044319 (2003).